

# Blue-Emitting Butterfly-Shaped 1,3,5,9-Tetraarylpyrenes: Synthesis, Crystal Structures, and Photophysical Properties

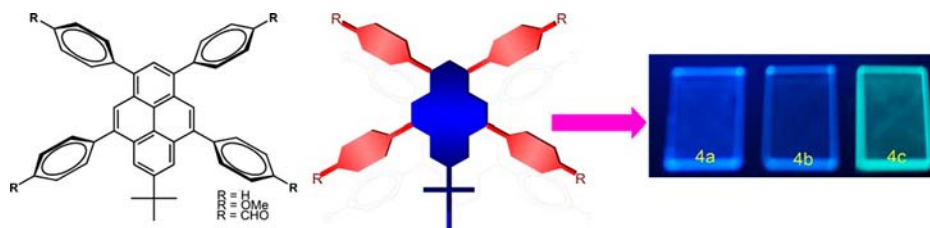
Xing Feng,<sup>†</sup> Jian-Yong Hu,<sup>\*,†,‡</sup> Fumitaka Iwanaga,<sup>†</sup> Nobuyuki Seto,<sup>†</sup> Carl Redshaw,<sup>§</sup> Mark R. J. Elsegood,<sup>||</sup> and Takehiko Yamato<sup>\*,†</sup>

Department of Applied Chemistry, Faculty of Science and Engineering, Saga University, Honjo-machi 1, Saga-shi, Saga 840-8502, Japan, Department of Organic Device Engineering, Yamagata University, Yonezawa, Yamagata 992-8510, Japan, Department of Chemistry, The University of Hull, Hull HU6 7RX, U.K., and Chemistry Department, Loughborough University, Leicestershire LE11 3TU, U.K.

yamatot@cc.saga-u.ac.jp; hujianyong@yz.yamagata-u.ac.jp

Received January 29, 2013

## ABSTRACT



The first example of aryl-functionalized, butterfly-shaped, highly fluorescent and stable blue-emitting monomers, namely, 7-*tert*-butyl-1,3,5,9-tetrakis(*p*-R-phenyl)pyrenes, were synthesized by the Suzuki–Miyaura cross-coupling reaction from a novel bromide precursor of 1,3,5,9-tetrabromo-7-*tert*-butylpyrene. The crystal structures and optical and electronic properties have been investigated.

The development of efficient optoelectronic materials based on polycyclic aromatic hydrocarbons (PAHs) has been extensively investigated in the past two decades.<sup>1</sup> Indeed, many members of PAHs have been employed in organic light-emitting diodes (OLEDs)<sup>2,3</sup> and other

optoelectronic devices,<sup>4</sup> as well as fluorescence probes.<sup>5</sup> Pyrene and its derivative are important members of PAHs that have exhibited several advantages: (1) solution processable, (2) good thermal stability, (3) enhanced charge carrier mobility, and (4) intense luminescence efficiency. However, the use of pyrenes as efficient emitters in OLEDs has been somewhat limited,<sup>2</sup> primarily because the planar structure of pyrene has a strong tendency to form  $\pi$ -aggregates/excimers, thereby quenching the fluorescence in concentrated solution or in the solid-state. To suppress the passive aggregation, several research groups have been focused on exploring the availability of methods for the functionalization of the pyrene core. In general, the 1-, 3-, 6-, and 8-positions of pyrene preferentially undergo electrophilic aromatic substitution ( $S_EAr$ ) reactions. Thus, various pyrene derivatives<sup>2</sup> (Supporting Information) can be easily accessed depending on the experimental conditions.<sup>6</sup>

<sup>†</sup> Saga University.

<sup>‡</sup> Yamagata University.

<sup>§</sup> The University of Hull.

<sup>||</sup> Loughborough University.

(1) (a) Havey, R. G. *Polycyclic Aromatic Hydrocarbons*; Wiley-VCH: New York, 1997. (b) Schmidt-Mende, L.; Fechtenkötter, A.; Müllen, K.; Moons, E.; Friend, R. H.; MacKenzie, J. D. *Science* **2001**, *293*, 1119–1122. (c) Richter, M. M. *Chem. Rev.* **2004**, *104*, 3003–3036.

(2) Figueira-Duarte, T. M.; Müllen, K. *Chem. Rev.* **2011**, *111*, 7260–7314.

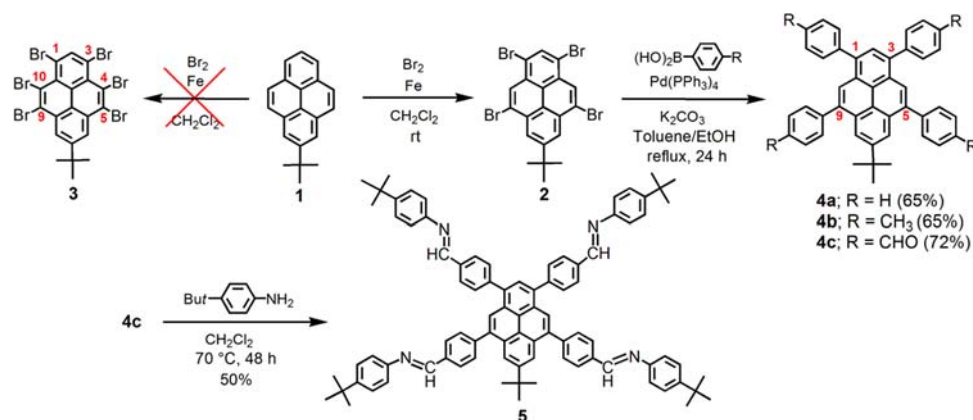
(3) Lo, M. Y.; Zhen, C.-G.; Lauters, M.; Jabbour, G. E.; Sellinger, A. *J. Am. Chem. Soc.* **2007**, *129*, 5808–5809.

(4) (a) Ashizawa, M.; Yamada, K.; Fukaya, A.; Kato, Reizo.; Hara, K.; Takeya, J. *Chem. Mater.* **2008**, *20*, 4883–4890. (b) Wen, Y.-G.; Liu, Y.-Q.; Guo, Y.-L.; Yu, G.; Hu, W.-P. *Chem. Rev.* **2011**, *111*, 3358–3406.

(5) (a) Goedeweck, R.; Vanderauweraer, M.; Deschryver, F. C. *J. Am. Chem. Soc.* **1985**, *107*, 2334–2341. (b) Ni, X.-L.; Zeng, X.; Redshaw, C.; Yamato, T. *J. Org. Chem.* **2011**, *76*, 5696–5702. (c) Ahmed, N.; Shirinfar, B.; Geronimo, I.; Kim, K. S. *Org. Lett.* **2011**, *13*, 5476–5479. (d) Lewis, F. D.; Zhang, Y. F.; Letsinger, R. L. *J. Am. Chem. Soc.* **1997**, *119*, 5451–5452.

(6) (a) Bernhardt, S.; Kastler, M.; Enkelmann, V.; Baumgarten, M.; Müllen, K. *Chem.–Eur. J.* **2006**, *12*, 6117–6128. (b) Vollmann, H.; Becker, H.; Corell, M.; Streeck, H. *Justus Liebigs Ann. Chem.* **1937**, *531*, 1–159.

**Scheme 1.** Synthesis of Compounds **4** and **5**



On the other hand, the 4-, 5-, 9-, and 10-positions (i.e., K-region) of the pyrene are facile to bromination in the presence of iron powder if the sterically bulky *tert*-butyl groups are located at the 2- and 7-positions.<sup>7</sup> Interestingly, on further prolonging the reaction time, the *ipso*-bromination product of 4,5,7,9,10-pentabromopyrene can be obtained.<sup>8</sup> Besides the electrophilic substitution of pyrene, Hu et al. reported an efficient, one-step synthetic approach to catalyze the oxidation of the K-region of pyrene using ruthenium chloride.<sup>9</sup> Müllen et al.<sup>10</sup> also developed an asymmetric functionalization method to direct bromination to the K-region of the pyrene without the protective *tert*-butyl groups. Recently, it was found that the active sites of the 1,3-positions of pyrene could be brominated from starting compound **1** because the *tert*-butyl group protects the ring from electrophilic attack at the 6,8-positions.<sup>11</sup> In addition, we reported the selective formation of the 5-mono- and 5,9-disubstitution products from 7-*tert*-butyl-1,3-dimethylpyrene by formylation and acetylation depending on the Lewis acid catalysts used.<sup>12</sup> Thus, based on the above-mentioned research, we attempted to exploit a new intermediate in order to develop a series of pyrene related materials for further applications. Our initial attempt was to synthesize 1,3,4,5,9,10-hexabromo-7-*tert*-butylpyrene (**3**) using iron powder to catalyze its formation from 2-*tert*-butylpyrene (**1**) in different solvents; however, efforts using CH<sub>2</sub>Cl<sub>2</sub>, nitrobenzene, and benzene all failed. Probably, the bromo atom substituted at the 1- and 3-positions of the pyrene would sterically hinder the 4- and 10-positions, thereby enabling regioselective substitution at the 5- and 9-positions. Since the 7-position of

the pyrene ring has been protected, four bromines atoms can be introduced at the 1-, 3-, 5-, and 9-positions by electrophilic bromination of 2-*tert*-butylpyrene (**1**). Herein, we succeeded in developing a new bromide precursor, 1,3,5,9-tetrabromo-7-*tert*-butylpyrene (**2**), in excellent yield (Scheme 1). To the best of our knowledge, this is the first example of a method to halogenate the pyrene ring both in the activated sites (1- and 3-positions) and in the K-region (5- and 9-positions).

The precursor **2** has two advantages: (1) the active sites at the 1- and 3-positions could give C-functionalized pyrene by the cross-coupling reaction to suppress the aggregation,<sup>11a,11a</sup> and (2) the K-region (5- and 9-positions) affords a strategy to extend conjugated systems to larger PAHs by cyclization.<sup>13</sup> Accordingly, in this study, by using **2** as an intermediate, we synthesized novel butterfly-shaped, highly fluorescent, and stable blue-emitting monomers, namely, 1,3,5,9-tetraaryl-7-*tert*-butylpyrenes (**4**), which were characterized by X-ray diffraction, absorption and fluorescence spectra, electrochemical data, and density functional theory (DFT).

As described in Scheme 1, the mono-*tert*-butylated product, 2-*tert*-butylpyrene (**1**),<sup>14</sup> treated with Br<sub>2</sub> (6 equiv) in CH<sub>2</sub>Cl<sub>2</sub> at room temperature in the presence of iron powder yielded the expected tetrabromopyrene **2** in a high yield of 84%. Then, Suzuki cross-coupling reaction of **2** with the corresponding arylboronic acids afforded the 1,3,5,9-tetraaryl-7-*tert*-butylpyrenes **4** in isolated yields of 65–72%. As a comparison, we synthesized the Schiff base **5** from the aromatic aldehyde **4c** (Scheme 1) and **6** [1,3,6,8-tetrakis(4-methoxyphenyl)pyrene] according to the reported literature procedure.<sup>15</sup>

The molecular structures of compounds **4**–**6** were characterized by <sup>1</sup>H/<sup>13</sup>C NMR spectra, single-crystal X-ray

(7) Yamato, T.; Fujimoto, M.; Miyazawa, A.; Matsuo, K. *J. Chem. Soc., Perkin Trans. 1* **1997**, 1201–1207.

(8) Hu, J.-Y.; Ni, X.-L.; Feng, X.; Era, M.; Elsegood, M. R. J.; Teat, S. J.; Yamato, T. *Org. Biomol. Chem.* **2012**, *10*, 2255–2262.

(9) Hu, J.; Zhang, D.; Harris, F. W. *J. Org. Chem.* **2005**, *70*, 707–708.

(10) Zöphel, L.; Beckmann, D.; Enkelmann, V.; Chercka, D.; Rieger, R.; Müllen, K. *Chem. Commun.* **2011**, 47, 6960–6962.

(11) (a) Figueira-Duarte, T. M.; Simon, S. C.; Wagner, M.; Druzhinin, S. I.; Zacharias, K. A.; Müllen, K. *Angew. Chem., Int. Ed.* **2008**, *47*, 10175–10178. (b) Feng, X.; Hu, J.-Y.; Yi, L.; Seto, N.; Tao, Z.; Redshaw, C.; Elsegood, M. R. J.; Yamato, T. *Chem.—Asian J.* **2012**, *7*, 2854–2863.

(12) Hu, J.-Y.; Paudel, A.; Yamato, T. *J. Chem. Res.* **2008**, 308–311.

(13) (a) Paudel, A.; Hu, J.-Y.; Yamato, T. *J. Chem. Res.* **2008**, 457–460. (b) Hu, J.-Y.; Paudel, A.; Seto, N.; Feng, X.; Era, M.; Matsumoto, T.; Tanaka, J.; Elsegood, M. R. J.; Redshaw, C.; Yamato, T. *Org. Biomol. Chem.* **2013**, *10*, 1039/C3OB27320B.

(14) Miura, N.; Yamano, E.; Tanaka, A.; Yamauchi, J. *J. Org. Chem.* **1994**, *59*, 3294–3300.

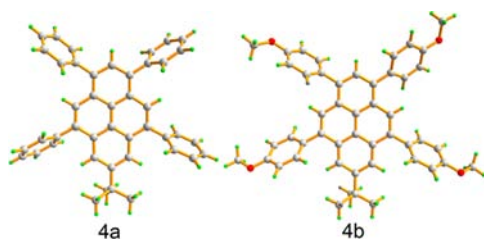
(15) Halleux, V. de.; Callbert, J.-P.; Brocorens, P.; Cornil, J.; Declercq, J.-P.; Brédas, J.-L.; Geerts, Y. *Adv. Funct. Mater.* **2004**, *14*, 649–659.

**Table 1.** Photophysical and Electrochemical Properties of Compounds **4**, **5** and **6**

compd	$\lambda_{\max}$ abs (nm) solns <sup>a</sup> /films <sup>b</sup>		$\lambda_{\max}$ PL (nm) solns <sup>a</sup> /films <sup>b</sup>		$\Phi_f^c$ solns/thin films	LUMO (eV)	HOMO (eV)	HOMO–LUMO $\Delta E$ (eV)	$T_m^d$ (°C)	$T_d^e$ (°C)
<b>4a</b>	373	380	412	410	0.92/0.75	−1.58	−5.01	3.43	335	350
<b>4b</b>	379	369	421	443	0.90/0.72	−1.36	−4.76	3.40	330	410
<b>4c</b>	386	400	469	471	0.56/0.48	−2.45	−5.66	3.21	302	329
<b>5</b>	355	nd	467	nd	nd/nd	−2.12	−5.25	3.13	266	430
<b>6</b>	391	405	434	488	0.94/nd	−1.47	−4.71	3.24	271	nd

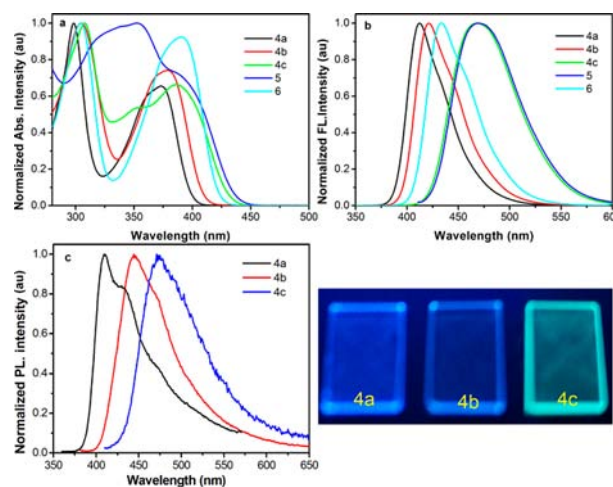
<sup>a</sup> Maximum absorption wavelength measured in dichloromethane at room temperature. <sup>b</sup> Measured in thin neat films. <sup>c</sup> Measured in dichloromethane and in neat thin films, respectively. <sup>d</sup> Melting temperature ( $T_m$ ) obtained from differential scanning calorimetry (DSC) measurement. <sup>e</sup> Decomposition temperature ( $T_d$ ) obtained from thermogravimetric analysis (TGA). nd: no determination.

diffraction, FT-IR spectroscopy, mass spectroscopy, as well as elemental analysis. All compounds **4** were soluble in common organic solvents such as toluene,  $\text{CH}_2\text{Cl}_2$ ,  $\text{CHCl}_3$ , THF, acetonitrile, and *N,N*-dimethylformamide (DMF) and exhibited excellent thermal stability under air/ $\text{N}_2$ . The key thermal data for the pyrenes **4** are summarized in Table 1.

**Figure 1.** X-ray structure of compounds **4a** and **4b**.

Single crystals of **4a** (CCDC 917256), **4b** (CCDC 917257), and **6** (CCDC 915429) were grown from a mixture of  $\text{CH}_2\text{Cl}_2$  and MeOH and investigated by X-ray crystallography to establish the structure. All crystal structures were found to belong to the monoclinic crystal system with space group  $P2_1/c$  for **4a** and **6** and  $P2_1/n$  for **4b**. As shown in Figure 1, these terminal moieties adopt a reasonably twisted conformation with a substantial dihedral angle relative to the pyrene ring ( $46.2$ – $68.0^\circ$ ), and torsion angles of  $49.4$ – $70.5^\circ$  between the pyrene and phenyl rings, while for the pyrene and methoxyphenyl rings, the torsion angles were  $48.1$ – $56.2^\circ$ . In compounds **4**, the four terminal moieties twist with reasonable dihedral angles relative to the pyrene cores by the proximal hydrogen atoms. This conformation effectively suppresses  $\pi$ – $\pi$  stacking and releases the steric interactions in the solid state. Only  $\text{C}–\text{H}\cdots\pi$  interactions were observed, and they impact on molecular geometries as well as prevent excimer formation in the solid state.<sup>16</sup> The packing of molecules of **4a** and **4b** revealed the 2D self-assembled planar

solid-state structure. However, the compound **6** exhibited a sandwich-like 3D structure self-assembled in the solid-state via  $\text{C}–\text{H}\cdots\pi$  bond interactions overlapping the porous two-dimensional networks. A chloroform molecule was encapsulated in the molecular channel by a hydrogen bonding  $\text{C45}–\text{H45}\cdots\text{O4}$  ( $2.506$  Å) interaction (see the Supporting Information).

**Figure 2.** (a) Normalized UV–vis absorption and (b) emission spectra of compounds **4** recorded in dichloromethane at ca.  $\sim 10^{-5}$ – $10^{-6}$  M at  $25^\circ\text{C}$ . (c) Emission spectra of **4** in thin film (d) photographs of blue emission from the films of **4** (left  $\rightarrow$  right).

The UV absorption and fluorescence spectra of **4**–**6** were investigated in dichloromethane and in a thin film (Figure 2). For **4a**–**c** and **6**, two prominent absorption bands were observed in between  $298$ – $308$  nm and  $373$ – $391$  nm, and the absorption spectrum of **4c** was broader and less well-resolved in the range of  $330$ – $420$  nm. The compounds **4** have a slight red-shift order of **4c** (CHO)  $>$  **4b** (OMe)  $>$  **4a** (H), which are in agreement with our previous reports.<sup>8,11b</sup> For the Schiff base **5**, the broader absorption spectrum was observed at  $355$  nm, arising from the more delocalized chromophore (red shift) with a possibility for charge transfer (broadened spectrum). In the thin film absorptions (Table 1 and Supporting

(16) (a) Würthner, F.; Thalacker, C.; Diele, S.; Tschierske, C. *Chem.–Eur. J.* **2001**, *7*, 2245–2253. (b) Jenekhe, S. A.; Osaheni, J. A. *Science* **1994**, *265*, 765–768.



Information), the compounds **4** have slightly broader spectra with red-shifts (5–14 nm) in comparison to that observed in solution, which can be explained by re-absorption in the solid-state. For **6**, however, an unusual zigzag-type absorption spectrum was observed with a maximum at 391 nm, indicating its trend to form a single crystal in the solid state causes a high noise level.<sup>15</sup>

Upon excitation, the emission maxima at 412 nm for **4a** and 421 nm for **4b** reveal a smaller red shift than compound **6** ( $\lambda_{\text{max}} = 434$  nm). For **4c** and **5**, however, the presence of the CHO moiety and the 4-*tert*-butylphenyl iminophenyl group caused a significant red-shift and a broadened emission maximum ( $\lambda_{\text{max}}$ ) at 469 and 467 nm, respectively. Nevertheless, no excimer emissions were observed in these newly developed butterfly-shaped tetraarylpyrene systems. The thin-solid film fluorescence spectrum of **4** presented a prominent maximum emission in the blue region at 410 nm for **4a**, 443 nm for **4b**, and 471 nm for **4c**, respectively. Interestingly, the emission spectrum of **4a** shows a slight hypsochromic shift with respect to the spectrum in solution. This difference might be due to the different dielectric constants.<sup>17</sup> Compound **4b** displayed a slight red-shift (~22 nm) compared to the spectra recorded in solution (Table 1), thought to be due to the aggregation. For **4c**, there is a slight red-shift (increased by 2 nm) in solution versus thin film. However, the fluorescence emission spectrum of **6** showed broad emission bands at 488 nm in the solid state. A 54 nm red-shift was observed with respect to the solution without the *tert*-butyl group. The substituents at the 5,9-positions of pyrene gave the structure more symmetry and played a key role for influencing  $S_1 \leftarrow S_0$  excitation.<sup>18</sup> Furthermore, parts b and c of Figure 2 revealed that these *butterfly*-shaped compounds **4** emit very bright, sharp, and solid-state blue fluorescence. All compounds **4** have very high quantum yields ( $\Phi_f^c$ ) in range of 0.56–0.92 in solution and 0.72–0.78 in the solid-state, respectively (Table 1). There is thus potential for these to be used as efficient blue emitters in OLEDs.

DFT calculations for **4–6** were performed using the Gaussian 03 program. The calculated density surfaces of the highest occupied molecular orbital (HOMO) and the lowest unoccupied molecular orbital (LUMO) of **4a**, **4c**, and **5** are shown in Figure 3 and the Supporting Information. The HOMO is located over the entire pyrene framework in each molecule, whereas the aryl substituent groups or extended chains have limited contributions to this system. However, it is remarkable that the LUMO of **4c** spreads over the entire pyrene framework, including the 4-formylphenyl unit. It is noteworthy that the terminal phenylimino groups do not contribute to the construction of the LUMO in **5**, despite of the introduction the extended  $\pi$ -conjugated by C=N bond.

The electrochemical properties of **4** were investigated by cyclic voltammetry (CV). All compounds showed

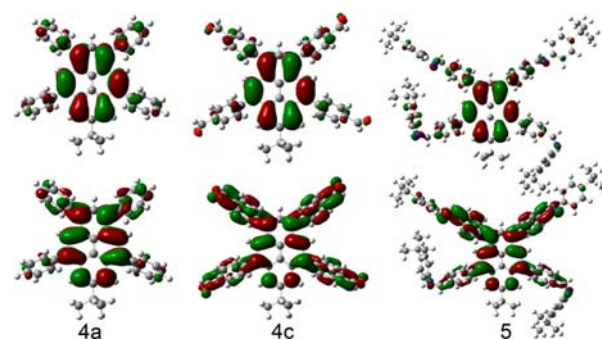


**Figure 3.** Spatial distributions of the compounds **4a**, **4c**, and **5** frontier orbitals. The lower plots represent the HOMOs, and the upper plots represent the LUMOs.

oxidation waves located at 1.48 V for **4a**, 1.35 V and 1.73 V for **4b**, and 1.75 V for **4c** (vs Fc/Fc<sup>+</sup>). All compounds displayed oxidation waves originating from the conjugation system of pyrene. The HOMO energy levels were calculated to be –5.49 eV for **4a**, –5.36 eV for **4b**, and –5.73 eV for **4c**, respectively, from the onset of the first oxidation wave. The energy gap ( $E_g$ ) was estimated from UV–vis absorption (3.11 eV for **4a**, 3.01 eV for **4b**, and 2.88 eV for **4c**). The experimental data was found to closely correspond to the theoretically calculated data (see the Supporting Information). The slight difference was caused by the theoretical calculations performed in the gas phase. The high reversibility of their redox processes demonstrated that the butterfly-shaped pyrenes were stable and suggested that the current molecular design may be suitable for OLED-like optoelectronic devices.

In conclusion, this work provides a promising strategy to halogenate both at the active sites and in the K-region. We successfully developed a novel bromide precursor of 1,3,5,9-tetrabromo-7-*tert*-butylpyrene. With this tetra bromopyrene as a key starting material, butterfly-shaped, highly efficient blue-emitting pyrene derivatives were synthesized. Both single-crystal X-ray analysis and photophysical properties for these pyrenes have been fully investigated. Further investigation of their applications in OLEDs is in progress in our laboratory.

**Acknowledgment.** This work was performed under the Cooperative Research Program of “Network Joint Research Center for Materials and Devices (Institute for Materials Chemistry and Engineering, Kyushu University)”. We thank the EPSRC (overseas travel grant to C.R.) and The Royal Society for financial support.

**Supporting Information Available.** Detailed descriptions of experimental procedures, X-ray crystallographic data, NMR data, and DFT. This materials is available free of charge via the Internet at <http://pubs.acs.org>.

The authors declare no competing financial interest.

(17) Tyagi, P.; Venkateswararao, A.; Thomas, K. R. J. *J. Org. Chem.* **2011**, *76*, 4571–4581.

(18) Crawford, A. G.; Dwyer, A. D.; Liu, Z.-Q.; Steffen, A.; Beeby, A.; Palsson, L.-O.; Tozer, D. L.; Marder, T. B. *J. Am. Chem. Soc.* **2011**, *133*, 13349–13362.